Orbit and Attitude Performance of the LightSail 2 Solar Sail Spacecraft

Justin R. Mansell* and David A. Spencer†
Purdue University, West Lafayette, IN, 47907, U.S.A.

Barbara A. Plante‡
Boreal Space, Moffett Field, CA, 94035, U.S.A.

Michael A. Fernandez§, Cole T. Gillespie¶, and John M. Bellardo‖
California Polytechnic University, San Luis Obispo, CA, 93407-0354, U.S.A.

Alex Diaz**
Ecliptic Enterprises, Moffett Field, CA, 94035, U.S.A.

Bruce Betts†† and Bill Nye‡‡
The Planetary Society, Pasadena, CA, 91101, U.S.A.

The Planetary Society's LightSail 2 satellite was launched June 25th, 2019, and has successfully demonstrated controlled solar sail propulsion using a CubeSat for the first time. This paper presents an assessment of the spacecraft's attitude determination and control performance along with the resulting changes in its orbit due to controlled solar propulsion. The results of on-orbit testing, important anomalies, and ongoing activities are also discussed. We conclude by offering lessons learned.

I. Introduction

SOLAR SAILS were first conceived by Johannes Kepler and have been imagined in fiction from Jules Verne to Arthur C. Clarke [1]. The concept of solar sailing is to use radiation pressure from the Sun to provide propellantless propulsion for spacecraft. Maxwell's equations of electromagnetism and later theories gave such ideas a sound physical basis, but it was not until the 21st century that the first solar sail would be realized. In 2005, the non-profit and member supported The Planetary Society attempted to fly Cosmos 1, a 100 kg spacecraft with a 600 m^2 solar sail, but the satellite was destroyed when the launch vehicle failed to reach orbit [1]. A NASA CubeSat solar sail, NanoSail D, was also lost in a launch failure in 2008 [2]. Successful solar sailing was finally achieved by the JAXA spacecraft, IKAROS, in 2010 [3]. The spacecraft was deployed on a heliocentric orbit and demonstrated acceleration and attitude control using solar radiation pressure. It had a mass of 306 kg and a 196 m^2 sail. NASA's 4 kg NanoSail D2 deployed a 10 m^2 solar sail in Earth orbit the following year but did not attempt controlled propulsion [4].

CubeSats are ideal for solar sailing due to their low mass. Following the loss of Cosmos 1, The Planetary Society reevaluated their solar sailing program and created the LightSail program. The new program raised $7 million USD over 10 years from 50,000 members and donors worldwide to develop a pair of 3U CubeSats to meet the following objectives:

- Demonstrate controlled solar sail propulsion using a CubeSat platform
- Raise the public and technical profile of solar sailing
- Excite and engage the public
- Share the program results with future missions, the technical community, and the public

---

*PhD Candidate, School of Aeronautics & Astronautics, 701 W Stadium Ave, West Lafayette, IN 47907 (jmansell@purdue.edu)

†Associate Professor, School of Aeronautics & Astronautics, 701 W Stadium Ave, West Lafayette, IN 47907

‡Founder and President

§Undergraduate Student

¶Undergraduate Student

‖Professor, Department of Computer Science

**Avionics Engineer

††LightSail Program Manager

‡‡Chief Executive Officer

Each of these satellites has a mass of 5 kg and carries a 32 m^2 Mylar solar sail. Since the characteristic acceleration of a solar sail depends on the ratio of the mass to sail area, the LightSail satellites have the highest solar acceleration of any solar sail yet flown.

LightSail 1 flew as a test mission in 2015 [5]. The mission was dedicated to check-out of CubeSat platform and validating deployment of the solar sail in space. These were accomplished with successful sail deployment occurring on June 7th, 2015. However, due to the low orbit altitude (356 km × 705 km), the spacecraft was quickly pulled from orbit by atmospheric drag and reentered the atmosphere on June 14th, 2015.

The experience gained from LightSail 1 resulted in a number of hardware and software changes for LightSail 2. Whereas LightSail 1 was uncontrolled, LightSail 2 incorporates a complete Attitude Determination and Control System (ADCS). This allows the spacecraft to control its orbit by changing the orientation of its sail relative to the Sun. To better observe the effects of solar pressure, the spacecraft was also carried to a higher orbit as part of the SpaceX STP-2 mission launched on June 25th, 2019. LightSail 2 was deployed from its carrier spacecraft, Prox 1, on July 3rd, 2019, into a 709 km × 726 km altitude orbit at 24 degrees inclination.

This paper presents an assessment of the on-orbit check-out and successful controlled solar sailing that followed. Section II reviews the spacecraft's ADCS hardware and software as well as the mission's concept of operations. Section III presents the results of key check-out tests performed on-orbit and characterizes the accuracy of attitude determination. Section IV assesses attitude control performance with the sail deployed, discusses key updates to solar sailing operations, and quantifies the effect of solar sailing on the evolution of LightSail 2's orbit. Section V discusses several important ADCS anomalies that were encountered during testing and solar sailing, Finally, Section VI presents lessons learned and discusses ongoing and planned future operations.

II. Attitude Determination and Control Overview

This section summarizes the ADCS hardware and software of LightSail 2. Previous papers describe the system in more detail [6]. The general configuration of the spacecraft and placement of the sensors is depicted in Figure 1.

| (a) Flight unit | (b) Sensor placements and body axes |
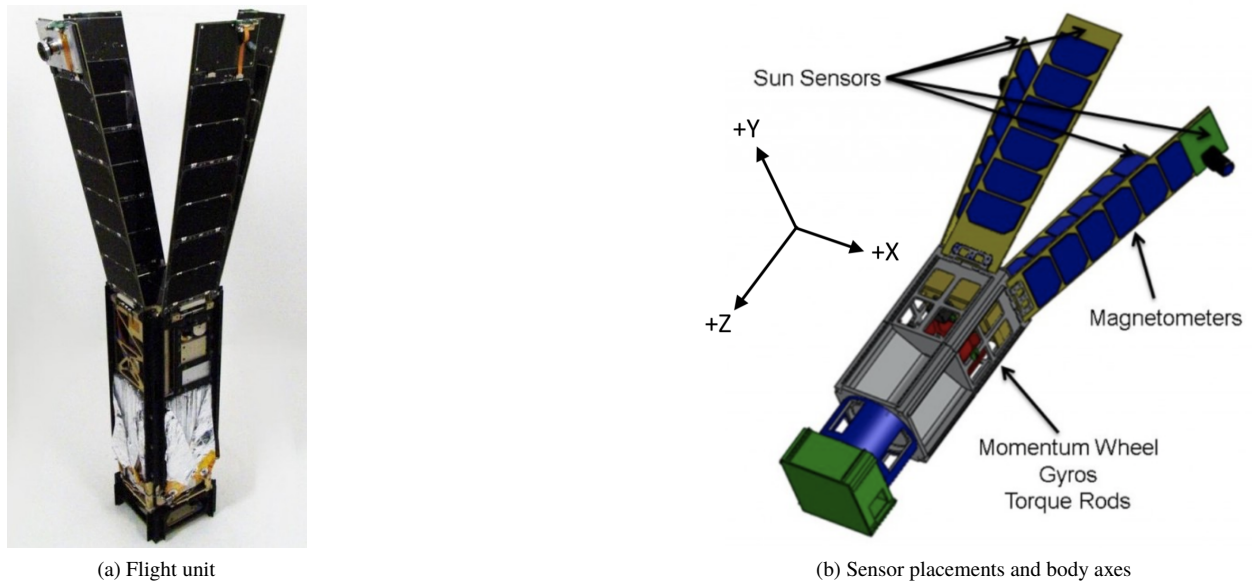
Fig. 1   Configuration of the LightSail 2 spacecraft

A. System Overview

Attitude control of LightSail 2 is accomplished using three magnetic torque rods (one for each axis) and a momentum wheel. The momentum wheel rotates about the +Y axis of the spacecraft and allows slews about this axis to be conducted rapidly. Attitude knowledge is provided by two 3-axis magnetometers on the +X and +Y solar panels and supplemented by a suite of four sun sensors located on ends the deployable solar panels plus one additional sun sensor on the -Z face.

Sun sensor measurements are voted on by transforming the measured sun vectors into the spacecraft body frame and comparing each measurement to the mean. Accepted measurements are incorporated into a discrete time multiplicative extended Kalman filter (EKF) to estimate the spacecraft attitude quaternions in the J2000 Earth-Centered Inertial (ECI) frame. Angular rate measurements are obtained from two sets of three gyros. The first set is an integrated sensor on the spacecraft's motherboard and provides limited accuracy. When accurate attitude determination and control is required, the second set of primary (PIB) gyros are used to provide an accuracy better than 1 deg/s. Two wide-angle cameras located on opposite solar panels allow imaging of the solar sail and the Earth. Finally, position and velocity knowledge is provided to the spacecraft for guidance and attitude determination in the form of two-line elements (TLE) that are uplinked and propagated by an onboard orbit propagator. New TLEs are uplinked to the spacecraft every few days depending on the quality of tracking and uplink/downlink priorities. The solar sail itself is composed of four triangular sheets of Mylar extended by 4 m booms upon deployment. Additional details are summarized in Table 1.

Table 1   ADCS hardware

Component	Manufacturer
Magnetometers	Honeywell
Sun sensors	Elmos
Primary gyros	Analog Devices
Momentum wheel	Sinclair Interplanetary
Magnetorquers	Stras Space
Detail	
Sail area	32 m^2 (square)
Volume of spacecraft bus	3U ($10 \times 10 \times 30$ cm)
Mass	4.93 kg

The ADCS software includes 6 operation modes:
- Mode 0: Detumble. Magnetometer readings are converted into the spacecraft body frame and B-dot control is used to generate torque rod commands to oppose the spacecraft's rotation. The PIB gyros and momentum wheel are not used.
- Mode 1: Magnetic alignment. The Z-axis torque rod is set to constant maximum power while the others act as in the detumble mode. This approximately aligns the +Z axis with the local magnetic field vector. The PIB gyros and momentum wheel are not used.
- Mode 2: Solar sailing. The PIB gyros and momentum wheel are powered on and LightSail 2 slews between thrusting and edge-on attitudes relative to the sun as described in Section II.B.
- Mode 3: No torques. All actuators and the PIB gyros are powered off.
- Mode 4: Unused.
- Mode 5: Velocity pointing. Currently unused.

B. Solar Sailing Concept of Operations

The goal of LightSail 2 is to demonstrate controlled solar sail propulsion by raising the spacecraft's orbit. Orbit raising is controlled by a cycle of "On-Off" slews about the spacecraft Y axis that switch the sail orientation between edge-on and thrusting attitudes twice per orbit as illustrated in Fig. 2. When the spacecraft is moving away from the Sun, LightSail 2 points the sail normal vector (+Z) directly away from the Sun. This is the "On" attitude and is intended to maximize the solar radiation pressure on the sail and ensure that the projection of the thrust onto the orbital velocity is positive. On the other half of the orbit, the "Off" or edge-on attitude is adopted to minimize thrust from the sail. In this way, the "On-Off" control scheme contributes an increase in the orbital energy that can oppose losses due to atmospheric drag.
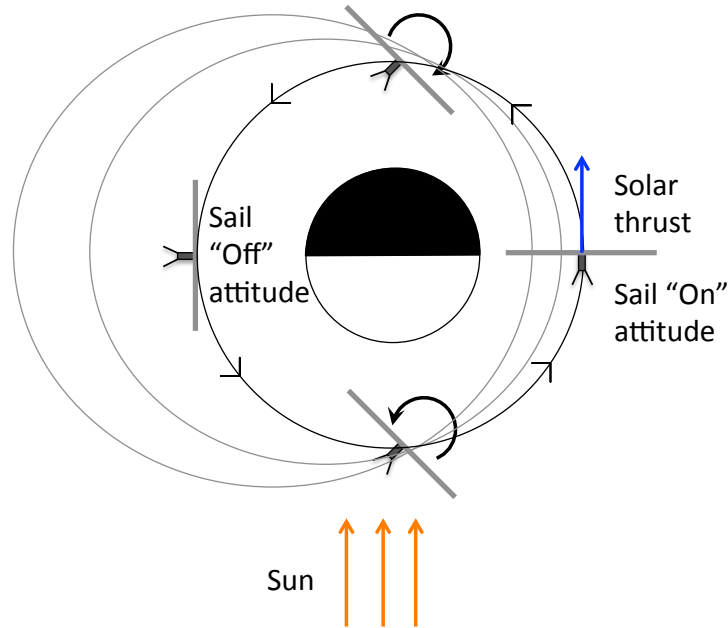
Fig. 2   Orbit raising strategy for LightSail 2. When moving away from the Sun the spacecraft presents the maximum sail area to the Sun to deliver an increase in the orbital energy. On the opposite arc, LightSail 2 transitions to an edge-on attitude to minimize solar pressure and prevent the sail from removing energy.

III. On-Orbit Testing

LightSail 2 began transmitting 45 minutes after its deployment from Prox 1. The Morse code identifier was received at 04:34:50 Eastern daylight time on July 3rd at the Cal Poly tracking station. Initial check-out activities focused primarily on LightSail 2's electrical and telecom systems. Prior to solar panel deployment, sun sensor and magnetometer measurements were unreliable due to these sensors being stowed internally to the spacecraft. Only once the panels were deployed on July 6th could the majority ADCS testing begin. Table 2 summarizes the timeline of critical ADCS events and check-out activities prior to solar sail deployment. The following subsections present the results of several key tests that confirmed the expected ADCS behavior.

Table 2   Major ADCS events prior to sail deployment

Date	ADCS Events/Testing
July 3	Deployment from Prox 1
July 6	Momentum wheel test and solar panel deployment
July 8	+Y magnetometer taken offline, successful mode 1 alignment
July 9-13	Multiple parameter and software updates
July 13	Successful detumble
July 14-17	Sensor software updates
July 14-22	Mode 2 testing, control parameter tuning and software updates
July 22	Successful mode 2 test

4

A. Sensor Validation

1. Magnetometers

Magnetometer readings were initially saturated due to the close proximity of the sensors to the spacecraft bus. Upon solar panel deployment the magnitudes agreed with the 2010 International Geomagnetic Reference Field (IGRF) at LightSail 2's orbital altitude. However, the direction of the measurements from the two sensors differed greatly and inconsistently when transformed into the spacecraft body frame. To determine which sensor was correct we capitalized on the approximately known orientation of the spacecraft in mode 1. In this mode the spacecraft's Z-axis will precess about the local magnetic field vector. A correct magnetometer should therefore show the angle between the measured magnetic field and spacecraft Z-axis to be less than 90 degrees. Figure 3 shows the results of one of the early mode 1 tests. Note that an incorrect parameter led to a reversed magnetorquer current for this test, causing the spacecraft's -Z axis to align with the local magnetic field. Hence, an angle of greater than 90 degrees was expected and can be seen with the +X magnetometer in the plot during the period of mode 1. Based on this and other tests, the +Y magnetometer was taken offline on July 8th, 2019.
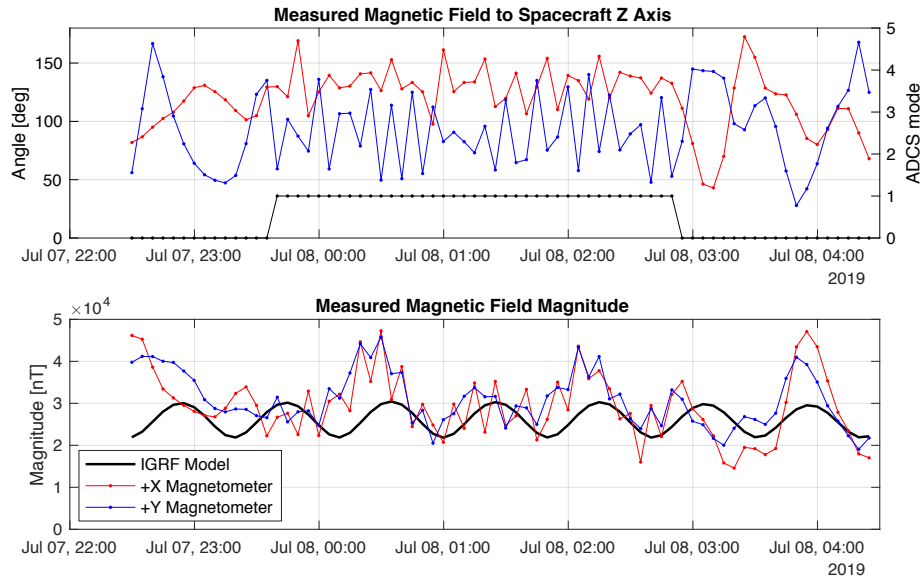

Fig. 3 On-orbit validation of the magnetometers was accomplished by placing the spacecraft in magnetic alignment mode. While both sensors gave consistent measurements of the magnitude of the magnetic field, only the +X magnetometer showed the expected alignment of the spacecraft with the magnetic field. Note that the standard error for the magnitude measured by the sensors is approximately 7750 nT.

2. Sun Sensors

The fields of view (FOV) of the five sun sensors are distributed about the -Z axis of the spacecraft with each FOV covering 165 degrees. The sensors do not discriminate based on the intensity of light source they are sensing and thus provide unreliable measurements in eclipse or any time the sun is not within their FOV. To improve robustness a voting scheme was implemented. Sun sensor measurements are transformed into the spacecraft body frame and averaged. Then, if any individual measurement differs from the average by more than the known 3-σ error of the sensors, that measurement is rejected for the current sample period (1 second). If more than half of the sensors are rejected in this way, the remaining sensors are also rejected. Separately from voting, sun sensors are also ignored when the spacecraft's propagated TLE indicates that it is currently in eclipse.

Downlinking the raw sun sensor measurements allows the voting process to be reconstructed on the ground. Figure 4 presents an example from later in the mission. The sun sensor measurements in this plot are seen to converge towards their average when the Sun approaches the -Z axis of the spacecraft. This is the expected behavior and shows that the sensors are correctly finding the Sun when it is visible. The +Y sensor is a clear outlier, however. This observation is

5

further supported by data collected over several days in Table 3 showing the fraction that each sun sensor was accepted during voting. Based on this analysis the +Y sensor was brought offline September 24th, 2019.
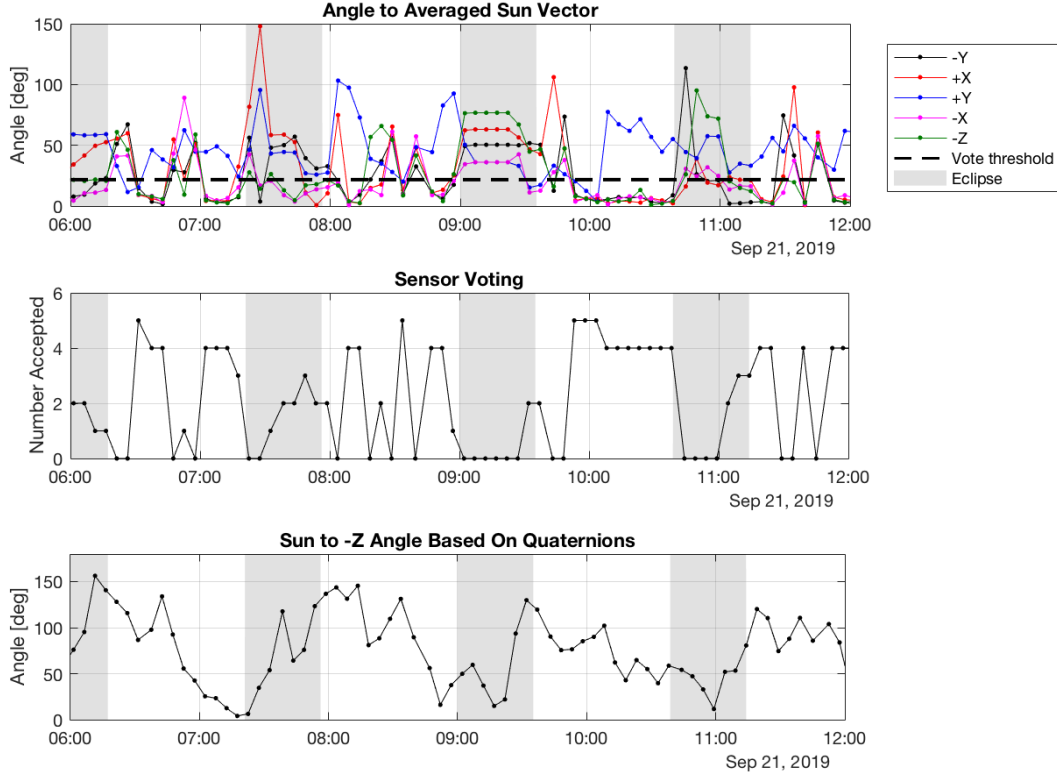
Fig. 4   Example validation of sun sensor performance. When the Sun to -Z angle is low, the sun should be visible to the sensors. The sensors correctly reach a high agreement on the sun vector at 07:00, 8:50, and 10:20 in the plot. Agreement at other times could be due to interference from other bright objects such as the Earth or Moon.

Table 3   Sun sensor voting statistics collected over several days in mid-September, 2019

| Sensor	-Y	+X	+Y	-X	-Z
Acceptance fraction	42%	43%	25%	43%	50%

B. Attitude Quaternion Validation

An important method of assessing the accuracy of LightSail 2's attitude quaternions was by comparing the measured direction of the magnetic field from the +X magnetometer with the predicted direction based on the IGRF model and estimated quaternion. If the quaternion is accurate the angular difference should be small. The process is as follows:

1) Compute the local magnetic field $\mathbf{B_{IGRF}}$ from the IGRF model at LightSail 2's position at the given time
2) Transform $\mathbf{B_{IGRF}}$ into the spacecraft body frame using the estimated attitude quaternion q
3) Transform $\mathbf{B_{+X}}$ from the +X magnetometer into the spacecraft body frame
4) Find the angular discrepancy between $\mathbf{B_{IGRF}}$ and $\mathbf{B_{+X}}$ in the spacecraft body frame

Figure 5 shows the angular difference during an early mode 2 test as well as for a longer period later in the mission. It is apparent from the figure that large discrepancies occur outside of mode 2, suggesting that the attitude estimate is unreliable in these modes. Considering only telemetry from mode 2, the mean angular discrepancy over the entire mission to date is 14.5 degrees, with the entire distribution pictured in Fig. 6. This serves as an upper bound for the

attitude determination error because, in addition to the estimation error, it includes the error of the magnetic field measurement. Given typical directional errors of 10 degrees for the magnetometer at LightSail 2's orbital altitude and IGRF errors of about 5 degrees, it is reasonable to conclude an attitude determination accuracy of approximately 10 degrees. Further confidence in the quaternions was achieved through analysis of sun sensor voting (Section III.A.2), trends in solar panel temperatures, and imaging.

(a) Pre-deployment solar sailing test

(b) Post-deployment solar sailing operations
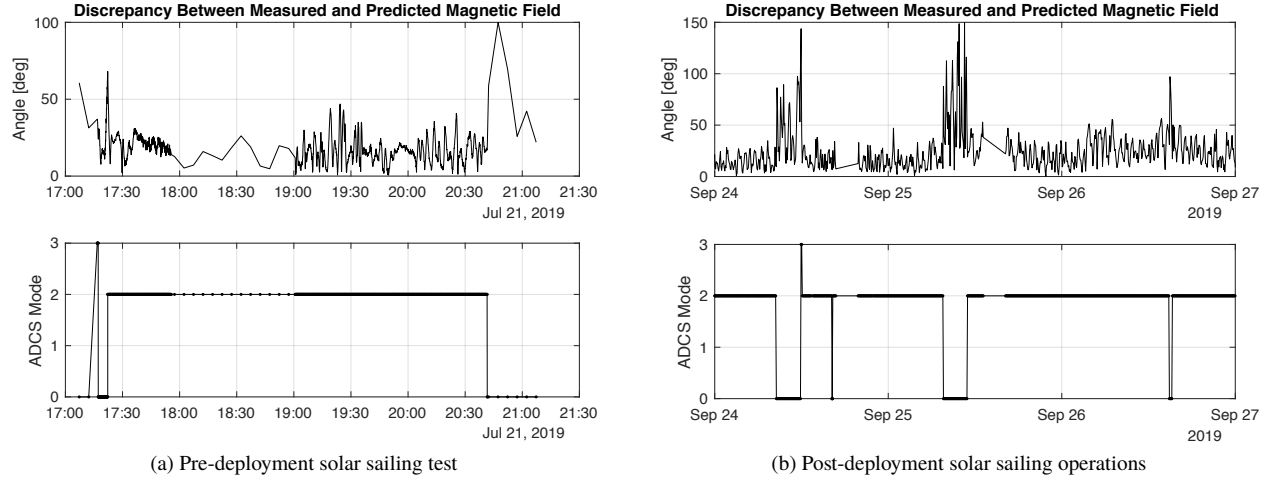
Fig. 5 Evaluation of the onboard attitude estimate for two periods during the mission. The predicted magnetic field vector is rotated into the spacecraft body frame using the estimated quaternion and compared with actual measurements. Large angular discrepancies indicate unreliable quaternions outside of solar sailing mode.
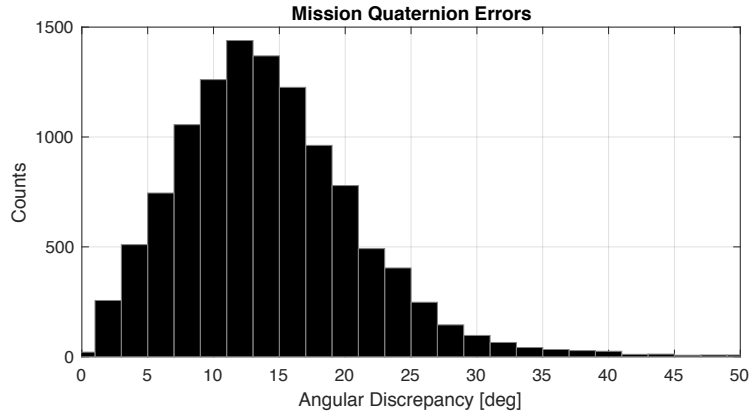
Fig. 6 Distribution of angular errors between the magnetic field predicted by the attitude quaternions and the actual 3-axis measurement. This distribution serves as an upper bound for the attitude determination accuracy.

The unreliable attitude estimates outside of mode 2 are due to these modes relying on the main board gyros rather than the more accurate PIB gyros. A significant and variable bias of several degrees per second for the z-axis main board gyro is present and could not be removed through cross-calibration with its PIB counterpart. The resulting bias destabilizes LightSail 2's attitude filter. Fortunately, this does not impact operations because these modes (0, 1, and 3) do not require attitude knowledge to function.
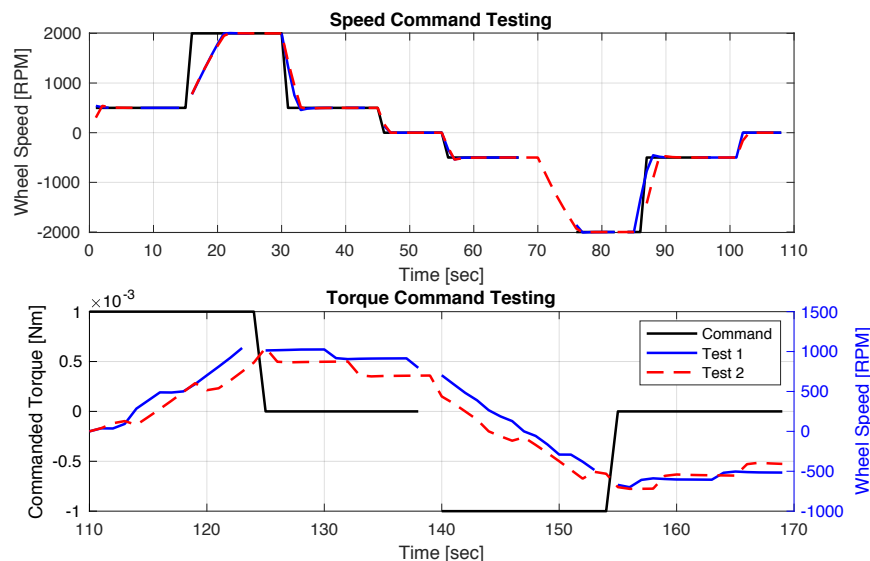
C. Momentum Wheel Testing
A significant precursor to solar sail deployment and entrance into solar sailing mode (mode 2) was the on-orbit checkout of LightSail 2's momentum wheel. Wheel behavior had previously been characterized during extensive ground

7

testing, but the mission operations team needed to understand if there were significant performance differences with the wheel when operating in zero gravity. This checkout activity, known as the autonomous wheel test, is a file-based set of manual wheel commands that can be initiated by ground command. When activated on July 6th, 2019, the autonomous wheel test exercised both commanded speeds and commanded torques in a prescribed, time-based sequence. The resulting data consisted of commanded and actuated values read directly from the wheel. The generated data was saved to a file and dowlinked for analysis.

A review of the downlinked test data showed behavior consistent with observations made during ground testing. In particular, when commanding speeds under 200 RPM, values read back from the wheel were often not in agreement with those commanded. Similarly, small commanded torque values at times resulted in zero torques being actuated. It was noted that, as observed on the ground, the wheel controller processed higher commanded speeds (>200 RPM) and torques more accurately than smaller ones. The resulting effect on later tests of mode 2 are discussed in Section V.

Results from the autonomous wheel test provided the mission operations team with confidence that the wheel was operating within expected parameters and that it would support spacecraft slews while solar sailing. A second autonomous wheel test was conducted on September 17th, 2019 to determine if wheel performance had changed since it was first characterized on-orbit. At the time of the second test, the wheel had been actuating in solar sailing mode for almost two months. Figure 7 shows no significant change in performance when either wheel speeds or wheel torques were commanded.

Fig. 7   Results of the first and second autonomous momentum wheel tests. In each test the wheel speed was first commanded directly. Then torques were commanded.

D. Mode 2 Testing

Testing of LightSail 2's solar sailing mode began on July 14, 2019. Initial tests were unsuccessful due to several software errors that led to anomalous performance of the momentum wheel (Section V.A). These errors were corrected by July 22nd, when the fourth and final pre-deployment mode 2 test took place. During this test, LightSail 2 correctly maneuvered between thrusting and edge-on attitudes as presented in Fig. 8. This figure shows the angle of the Sun with respect to the spacecraft -Z axis throughout the test.

IV. Solar Sailing Performance

Solar sail deployment was confirmed at 2:47 pm EDT on July 23, 2019 while LightSail 2 was passing over the continental USA. Prior to deployment the spacecraft was commanded into magnetic alignment mode (mode 1) for several orbits in order to provide good two-way communication and more direct lighting angles for imaging the sail. Deployment was performed in no-torques mode (mode 3) and lasted approximately 2 minutes. Figure 9 shows images
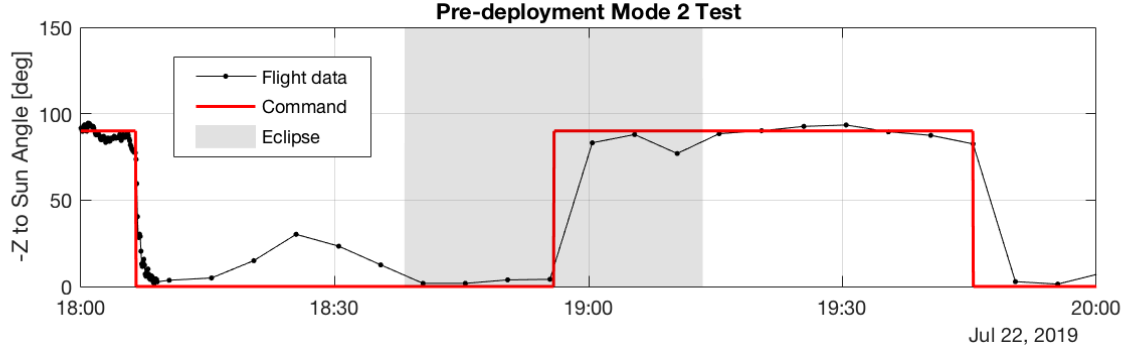
Fig. 8   The final solar sailing test prior to solar sail deployment. LightSail 2 successfully maneuvered between thrusting and edge-on sail attitudes.

captured by LightSail 2's cameras towards the end of the successful deployment.

Upon deployment, LightSail 2 automatically transitioned into solar sailing mode. Recognizable "On-Off" slews appeared in the telemetry on July 24th followed by saturation of the momentum wheel within several orbits. The flight team spent the next several days tuning the attitude control gains to balance performance with frequent momentum saturation events. Increases in orbit apogee also appeared soon after sail deployment. By July 29th the consistently increasing orbit apogee and visible on-off control led to the announcement of mission success.

Table 4 summarizes significant post-deployment milestones related to ADCS. The following subsections analyze LightSail 2's sail control in detail and describe strategies that were attempted for controlling the build up of angular momentum. The evolution of the spacecraft's orbit to date is also presented and the influence of controlled sailing on the orbit is quantified.
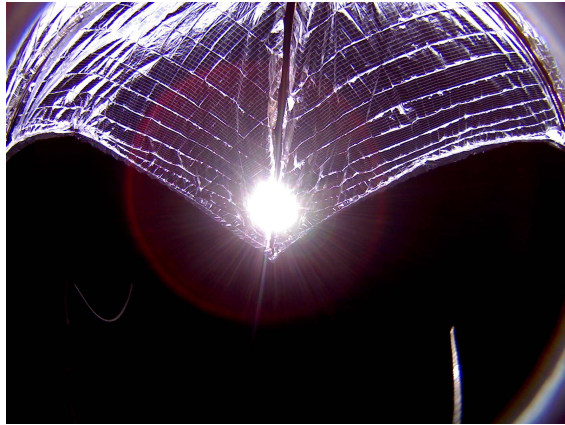

(a) Camera 1 (+X)
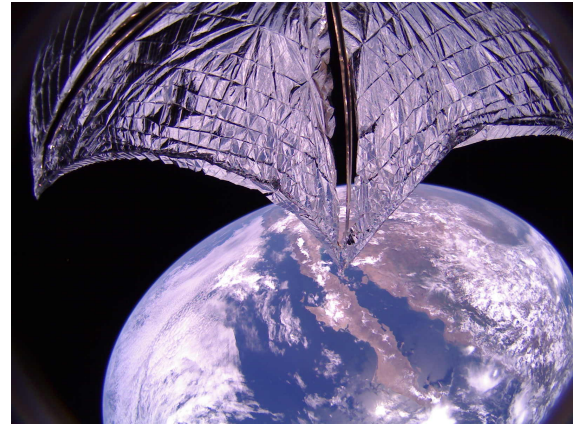
(b) Camera 2 (-X)

Fig. 9   LightSail 2's solar sail imaged during deployment on July 23rd, 2019

A. Sail Control

Precision attitude control is difficult due to the large moment of inertia of the deployed sail and the limited actuators of the CubeSat bus. Nonetheless, LightSail 2 has demonstrated extended periods of successful sail control throughout the mission. Figure 10 presents examples of continuous solar sailing over 12-hour periods from August, September, and October. Performance during these times is roughly consistent with pre-flight simulations. A process of trial-and-error was required to arrive at control gains that produced successful on-off control, as it was found that control gains which produced acceptable performance in simulation often did not lead to comparable results in flight. This is possibly due to the non-rigid dynamics of the sail, which is not accounted for in our simulations.

9

Table 4   Post deployment ADCS events

Date	ADCS Events/Testing
July 23	Solar sail deployment
July 24-28	Control parameter tuning, recognizable on-off slews
July 29	Apogee increase confirmed; mission success announced
August 1	Torque rod power increased, mode 1 eliminated
August 1-31	Control parameter tuning and new momentum desaturation strategies
August 29	Maximum apogee achieved
September 17	Second momentum wheel test
September 24	+Y Sun sensor deactivated
October 22	Minimum apogee reached
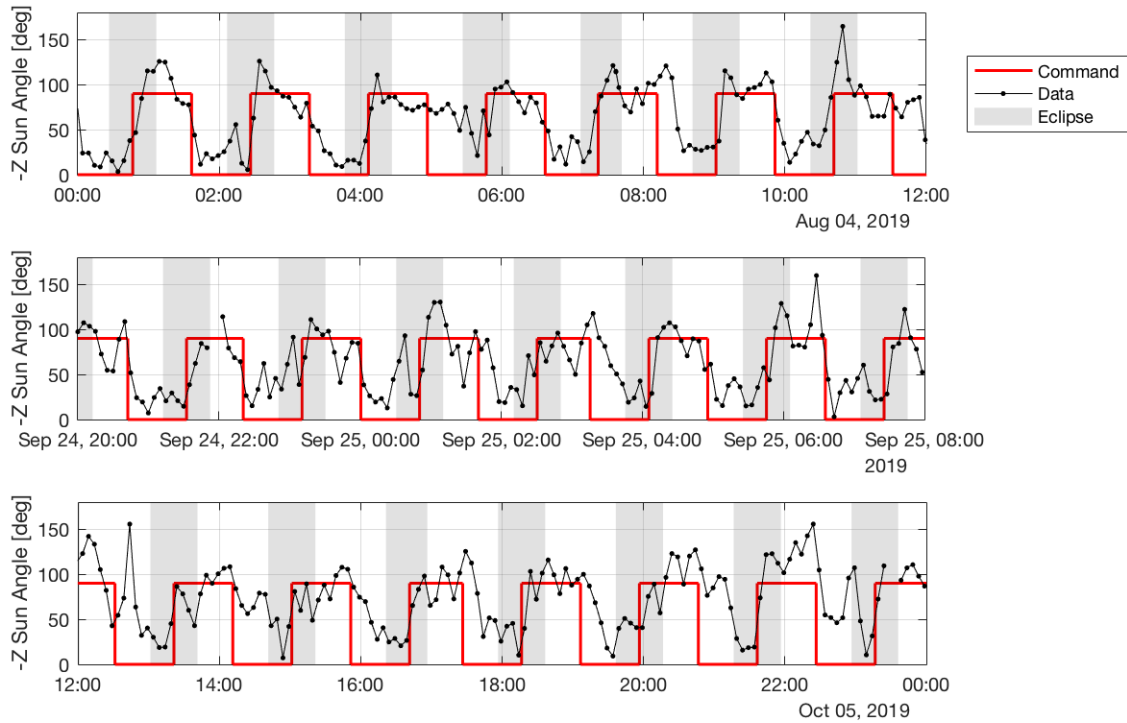
Fig. 10   Selected examples of continuous solar sailing operations. Despite the large inertia of the deployed sail, LightSail 2 is generally able to follow the commanded "on-off" profile.

Pointing accuracy has varied over the course of the mission in response to control parameter updates, new momentum management strategies, and anomalies. Figure 11 plots 24-hour averages of the pointing errors between the commanded "on-off" orientation and the actual -Z to Sun angle. Note that this plot does not account for the time required to slew between attitudes and therefore does not represent the steady-state pointing accuracy of the spacecraft. For comparison, a randomly oriented sail will have an average pointing error of 90 degrees for "on" attitudes and 45 degrees for "off" attitudes, for a total average error of 67.5 degrees.

Several days of good performance are present early in the mission, but were difficult to sustain due to frequent saturation of the momentum wheel. Throughout August, new momentum management strategies were tested. The torque rod commands were also increased by 50% to enhance attitude control and momentum dumping. Previously, the maximum dipole of the rods was limited to 0.66 Am^2 with a special exemption for the Z-axis torquer in mode 1, which was commanded to a constant 1.0 Am^2 in this mode. The relative increase in strength of the Z-axis torquer is what
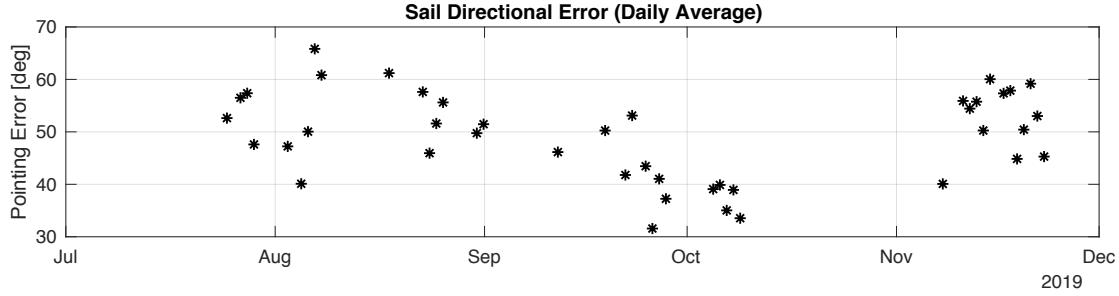
Fig. 11 Daily averages of sail pointing errors relative to the commanded -Z to Sun orientation. Control parameter refinements and improved momentum management led to improved performance throughout the mission.

causes the spacecraft to align its Z-axis with the local magnetic field in mode 1. Since this mode was no longer needed after sail deployment, we chose to scale all torque rod commands to a maximum of 1.0 Am^2, increasing their actuation power but effectively eliminating mode 1.

With these changes in place, a trend of improving performance is evident in Fig. 11 beginning in early September and continuing through early October as the momentum management strategy was refined and final tweaks were made to the control gains. By late September average on-off errors < 45 deg could be sustained over multiple days. The subsequent gap in the data is due to a lack of downlinked telemetry and extended periods spent outside of solar sailing mode due to the anomalies discussed in Section V.B. Sailing performance was reduced in November following this period as numerous software updates addressing these anomalies were prioritized over momentum management.

B. Momentum Management

Perturbation torques on the spacecraft lead to changes in LightSail 2's angular momentum. These changes can be opposed by the spacecraft's torque rods or absorbed by the momentum wheel. The momentum wheel does not directly counter the change in angular momentum but rather stores it by changing the wheel's rotational velocity. Eventually the wheel will reach its maximum rotational speed and will not be able to store further momentum. On LightSail 2 this occurs at a speed of 5920 RPM.

To remove the built-up angular momentum from the spacecraft, the momentum wheel is stopped and ADCS set to detumble mode. Stopping the wheel transfers the stored angular momentum back into the spacecraft body, causing it to spin, while detumble mode dampens the resulting rotation using the magnetic torque rods. Once the rotation is slowed, the momentum wheel can be turned on with a slower speed needed to absorb any remaining rotation. This process is referred to as momentum dumping or desaturation. In flight, several hours are typically required to completely desaturate LightSail 2's momentum wheel.

The frequency and length of momentum dumping periods greatly affects LightSail 2's solar sailing performance. If momentum is dumped too infrequently the spacecraft may experience long periods where attitude control is hindered by a saturated momentum wheel. On the other hand, LightSail 2 generally requires several orbits to stabilize its attitude after exiting detumble mode and frequent momentum dumping can interrupt the "on-off" maneuvers. Determining an appropriate duty cycle for momentum dumping is further complicated by the inconsistent rate at which the momentum wheel saturates.

Table 5 outlines the main momentum dumping strategies introduced during the mission. Figure 12 shows these strategies in action. Early after deployment the momentum wheel tended to saturate within a matter of hours. This was dealt with by manually commanding the spacecraft into detumble mode for one or more orbits as per the first strategy described in Table 5. Reduced control gains that slowed the slew rate helped reduce the rate of saturation, but this momentum management strategy still resulted in long periods where the momentum wheel was saturated.

The next strategy introduced a 4000 RPM threshold for triggering brief automatic desats. The goal was to prevent the wheel from saturating in the first place by incrementally removing momentum when the wheel speed was high. Though this was successful, the desats often triggered repeatedly and disrupted attitude control. During the rest of August several modifications to this strategy were trialed, including restricting the automatic desats to occur in eclipse and ramping the wheel speed down slowly so that the torque rods could counteract the braking torque. Unfortunately,

11

Table 5   Important momentum management strategies used during the mission

Strategy	Description	Introduced
Manual Desats	Manually command spacecraft into mode 0 for 1-2 orbits whenever wheel speed is observed to be at or near saturation	Jul. 25
RPM Threshold	Enter mode 0 for 10 minutes if wheel speed exceeds 4000 RPM	Aug. 3
Regular Desats	Manually command mode 0 for 2 orbits once per day regardless of wheel speed	Aug. 31
No torques	Command into no torques mode for 5 minutes prior to solar sailing to de-magnetize torque rods	Sep. 24

these did not offer significant improvements.

The most successful strategy has been to manually command a daily momentum dump two orbits in length. This is similar to the original strategy, but is performed irrespective of the wheel speed. In addition to limiting growth in the wheel speed, it also reduced the frequency of automatic desats and improved the overall control performance as shown in Fig. 11 and Fig. 12. The apparent improvement to sail control may be due to the removal of angular momentum about axes not actuated by the momentum wheel.

A further significant improvement in control performance was achieved by adding a 5-minute period in no-torques mode to the end of each regular desat. The sudden improvement is visible after September 24 in Fig. 11. The no-torques phase was added to potentially dissipate residual magnetic fields within the ferrite torque rod cores, which may have accumulated through sustained operation.
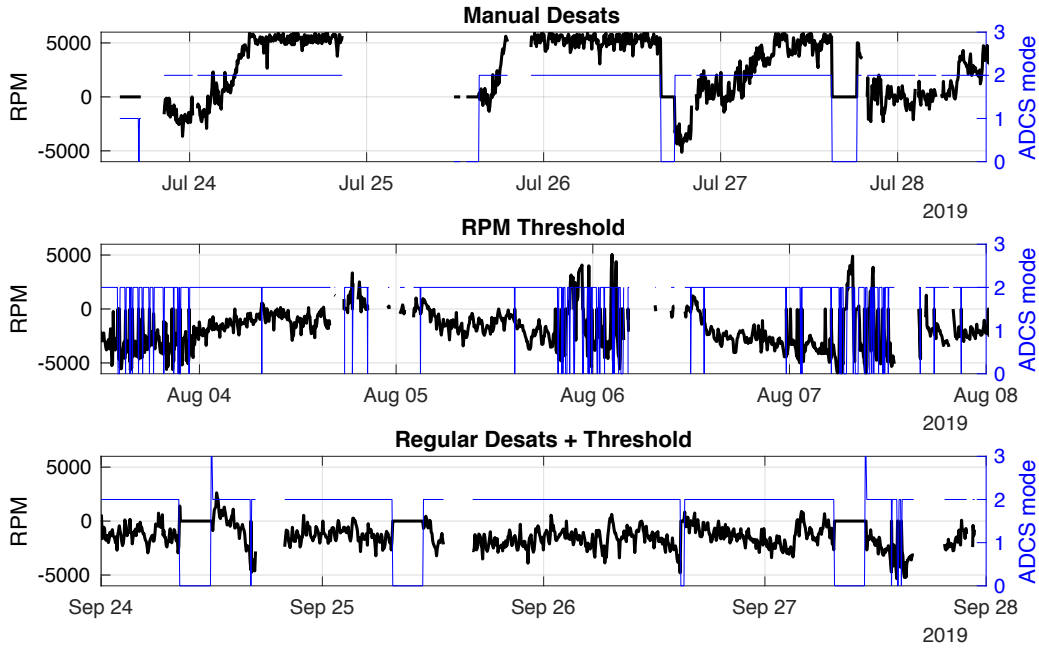
Fig. 12   Examples of the effectiveness of three of the main momentum management strategies for reducing saturation of the momentum wheel. Top: manual desats early after deployment left the satellite with a saturated momentum wheel much of the time. Middle: adding short automatic desats triggered by a 4000 RPM threshold helped reduced momentum build up but frequent desats disrupted attitude control. Bottom: the most successful strategy employed regular manually commanded desats and included a no-torques phase to demagnetize torque rods.

C. Orbit Evolution

Changes in LightSail 2's orbit have been monitored via publicly available TLEs provided by the 18th Space Control Squadron. The apogee and perigee altitudes of the orbit remained essentially constant prior to solar sail deployment. After sail deployment apogee began increasing while the perigee showed a mirrored decrease as shown in Fig. 13. These changes were expected given the initial orientation of the orbit relative to the Sun. At the beginning of August the line of apsides was nearly perpendicular to the Sun direction with the velocity at perigee pointed away as depicted in Fig. 14. In this orientation two effects conspire to decrease perigee. First, imperfect edge-on alignments between the sail and Sun during the "off" portion of the orbit lead to solar pressure acting against the spacecraft's velocity. This slows the spacecraft and reduces perigee. Second, solar thrust during the "on" portion of the orbit is downward relative to the local horizontal prior to perigee and upwards after it. Both of these also reduce perigee. At the same time, the energy increase from the thrust being aligned with the velocity speeds up the spacecraft and increases apogee.
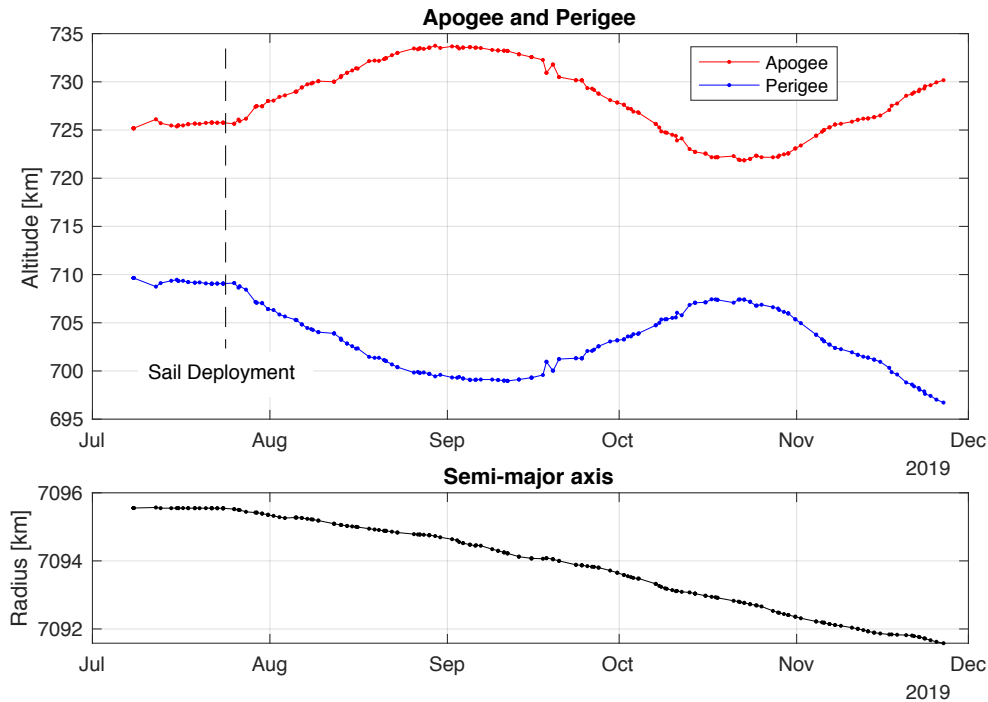

Fig. 13   Changes in the eccentricity and size of LightSail 2's orbit throughout the mission to date. After deployment, apogee and perigee oscillated in altitude while the semi-major axis trended downwards.

The angle of the line of apsides to the Sun changes over time due to perturbations (notably, the J_2 gravity harmonic from Earth's oblateness) and the rotation of Earth around the Sun. After approximately 2 months the line of apsides was again nearly perpendicular to the Sun but with apogee and perigee having switched places. This reversed the trend depicted in Fig. 14 so that apogee decreased while perigee increased due to solar pressure. By early November the orientation of the apisdes relative to the Sun returned to its original state, restoring the original trend of increasing apogee and decreasing perigee. Figure 15 provides a top-down view of the evolution of the orbit throughout the mission with the eccentricity highly exaggerated. The changing orientation of the orbit and the corresponding changes in eccentricity are clearly visible.

As the line of apsides continues to rotate, the oscillations in apogee/perigee are expected to persist. The overall size of the orbit, the semi-major axis, has trended downwards at varying rates due to atmospheric drag and on-off control performance. The contribution of controlled solar sailing to the orbit decay rate is assessed in the next subsection.

D. Effects of Sail Control

Unlike most other propulsion technologies, solar sails do not require an active effort to create thrust. Solar sails experience pressure along the sail normal vector any time they are exposed to sunlight. Though the magnitude and direction of the thrust varies depending on the orientation of the sail, this means that even an uncontrolled sail can
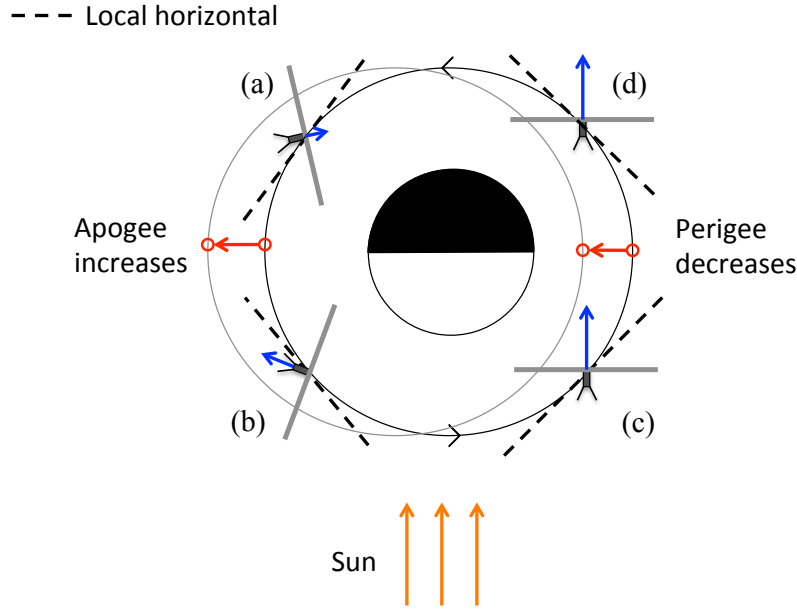
Fig. 14 Schematic of the orientation of the orbit relative to the Sun shortly after sail deployment. Changes in apogee and perigee mirror each other for several reasons. At (a) and (b) imperfect edge-on alignments between the sail and Sun reduce velocity and thus, perigee. At (c) the thrust of even a correctly oriented sail is downward relative to the local horizontal, reducing perigee. After perigee, at (d), the thrust is upward, also reducing perigee. However, at both (c) and (d) the sail thrust increases velocity, which raises apogee.

change its orbit using solar pressure. Attributing changes in the orbit to successful sail control is complicated by this as well as other factors. As discussed in Subsection IV.C, rates of change in apogee and perigee vary and even reverse depending on the orientation of the line of apsides to the Sun. Changes in the apsides are thus generally not comparable at different times. In addition to solar pressure, LightSail 2's orbit is also influenced by atmospheric drag, which is highly variable at LightSail 2's orbital altitude. Many data points must therefore be analyzed in order to average out these variations.

A better orbital parameter for judging the effects of sail control is the semi-major axis, since this is directly related to the spacecraft's orbital energy. By switching between thrusting and edge-on attitudes depending on whether LightSail 2 is moving away from or towards the Sun, the On-Off strategy allows solar pressure to provide a positive contribution the orbital energy. This contribution should be visible as a reduced rate of orbital decay.

Figure 16 presents two distributions of the changes in the semi-major axis between successive TLEs separated by at least 1 day. The black distribution is comprised of 32 intervals for which LightSail 2 remained entirely in an uncontrolled attitude mode (either detumble or no torques). The blue distribution is made up of 50 intervals during which the spacecraft was in solar sailing mode for at least 50% of the time but not more than 86%. The 86% cut-off is used to limit the data to intervals that include at least 2 full orbits per day of momentum dumping, since this proved crucial for effective sailing as discussed in Section IV.B. As is clear in Fig. 16, solar sailing results in a reduced rate of orbital decay. The difference between the average decay rates is −34.5 m/day for uncontrolled intervals versus −19.9 m/day for solar sailing, which is equivalent to a ΔV on the order of 1 cm/s. A two-sample Kolmogorov–Smirnov test confirms the independence of the two distributions with a confidence > 99%.

V. Anomalies

LightSail 2 encountered numerous ADCS anomalies both during on-orbit testing and later operations. This section describes several of the most important anomalies along with how they were resolved by the flight team.
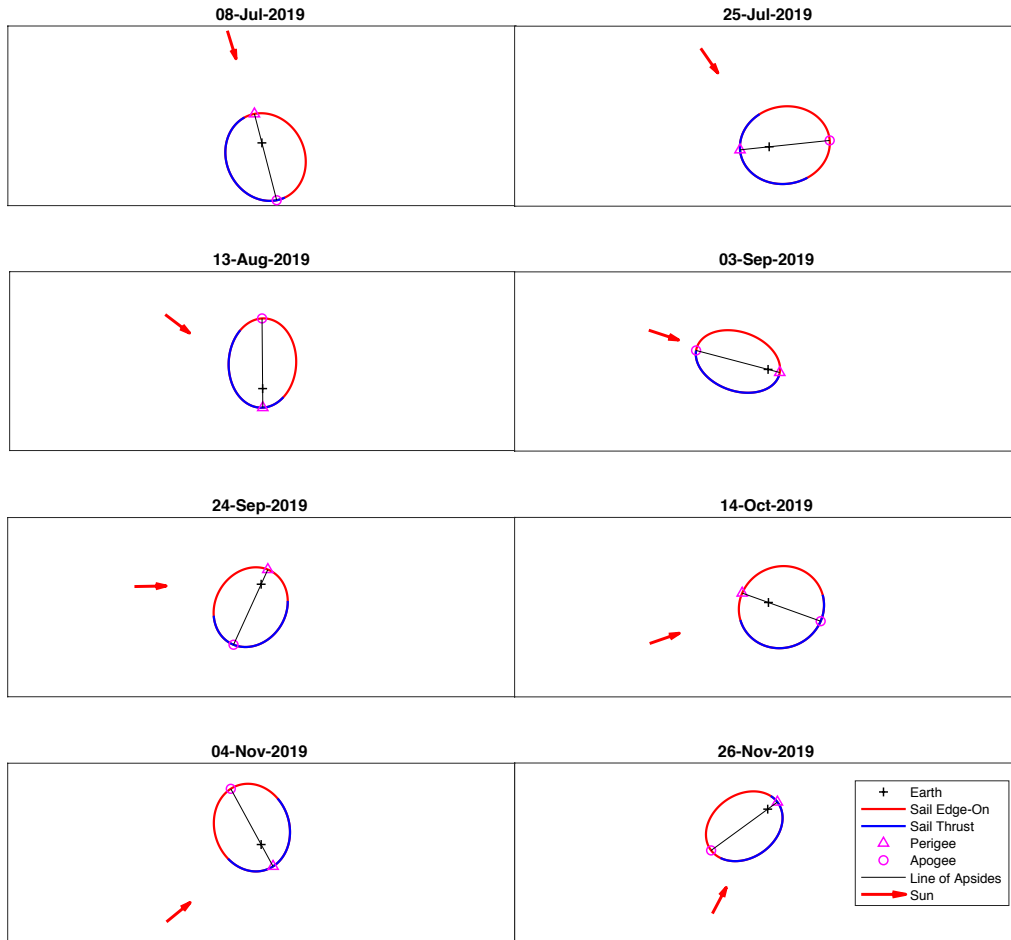
Fig. 15 The evolution of LightSail 2's orbit depicted top-down from Earth's axis with the orbital eccentricity highly exaggerated. The spacecraft follows the orbit counter-clockwise. Changes in eccentricity are greatest when the line of apisdes is perpendicular to the Sun.
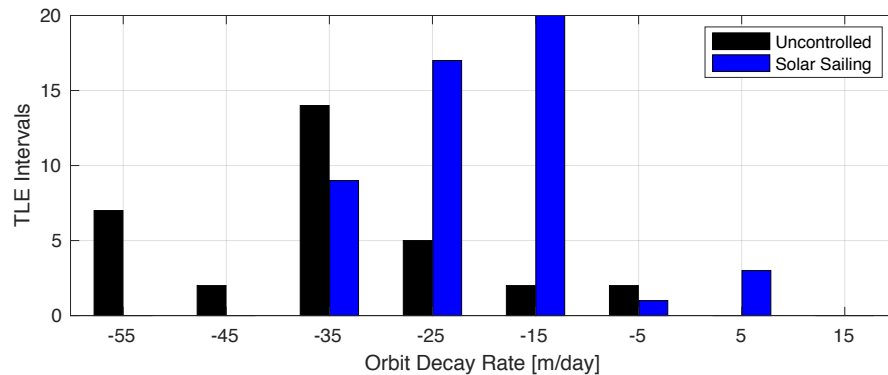
Fig. 16 The effect of solar sailing on LightSail 2's orbit decay. The chart shows the rate of change in orbital semi-major axis over successive two-line elements (TLEs) at least one day apart. Orbit decay is demonstrably reduced when LightSail 2 is conducting solar sailing.

A. Momentum Wheel Anomalies

Initial tests of mode 2 prior to sail deployment failed due to an apparently unresponsive momentum wheel. Inspection of the downlinked torque commands to the wheel showed that the commands were non-zero, yet the wheel speed remained unchanged except for brief pulses. We noted that the torque commands displayed significant chatter, as shown in Fig. 17, and theorized that the signal was too incoherent for the wheel motor to follow. A moving average filter was implemented to smooth the commands over a 10-second window and reduce noise, but this failed to rectify the problem on the subsequent test. In fact, it exasperated a second problem, which was that the magnitudes of the torque commands were generally too small to engage the wheel from a standstill. Averaging the torque commands thus led to even smaller magnitudes, and on the second mode 2 test the RPM remained almost entirely at 0. For the third test, attitude control gains were increased to produce torques $> 4 \times 10^{-4}$ Nm during slews after the moving average filter. This succeeded in engaging the wheel for sustained periods and revealed a final software error that prevented the wheel from reversing direction. After correcting this error the final mode 2 test was successful and the momentum wheel continues to perform nominally at the time of writing.
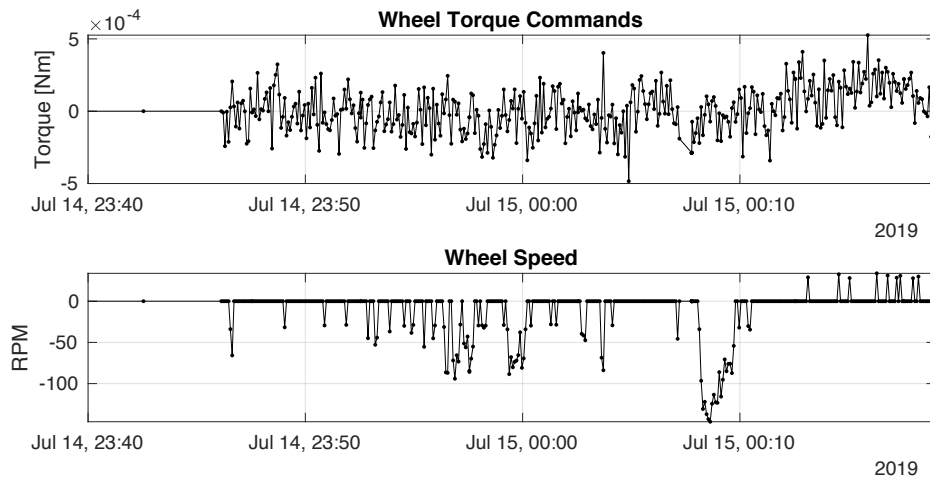
Fig. 17   Momentum wheel torque commands and RPM response during initial mode 2 testing. A combination of high chatter, low magnitudes, and a software error produced erratic behavior that inhibited attitude control.

B. ADCS Resets

A frequent problem that appeared beginning in mid-August were cyclic flight computer resets that interrupted solar sailing operations. Two examples are shown in Fig. 18. The causes of these resets were eventually traced down to two separate sources:

- Corrupt databases: Onboard telemetry databases can be corrupted by hard resets. If automatic attempts to repair the corruption fail, a watchdog timer reboots the flight computer.
- Battery under-volt: Many other resets correlated with low battery voltages and were likely the result of electrical brown-outs due to a low state of charge.

On-board telemetry is stored in databases that can become corrupted during hard resets caused by low power. Database corruption is detected automatically and attempts are made every hour to repair it. If the repair takes too long the process is ended by a watchdog timer. Three attempts are made, after which the watchdog timer reboots the spacecraft. This is why the reboots in the top plot of Fig. 18 occur exactly at 3-hour intervals. When this "saw-tooth" pattern of resets emerged, cycling the databases via a ground command was able to correct the issue.

Secondly, resets due to electrical brown-outs have often occurred during momentum dumping. This was initially perplexing because the detumble mode draws significantly less power than mode 2. Nevertheless, the tumbling attitude induced during momentum dumping leads to the solar sail routinely shadowing the solar panels. Solar sailing mode, on the other hand, provides superior battery charging by offering a stable Sun-facing attitude during the sail "on" phase of each orbit.

The frequency of electrical brown-outs reached a peak October 17-24 after a memory overload crashed the ADCS software and forced the spacecraft into a tumbling attitude for several days until memory could be freed. During this
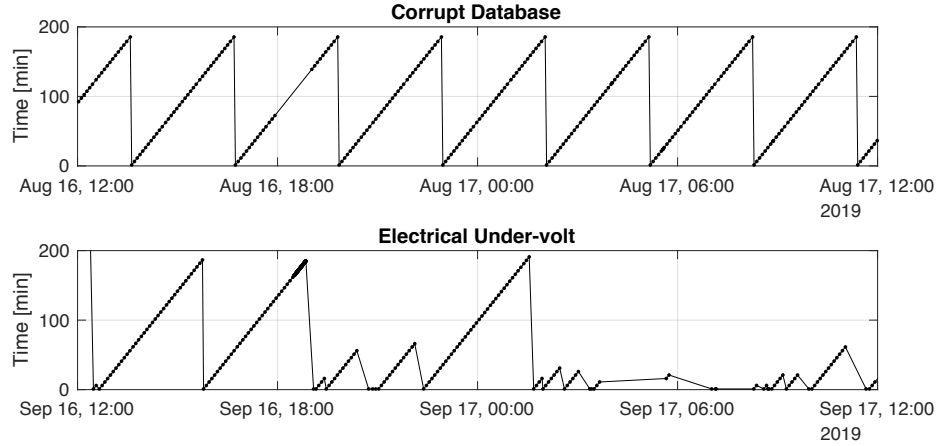
Fig. 18   Times since the last ADCS reboot with resets arising from two different causes. Top: a corrupt database causes resets with perfect regularity. Bottom: low battery voltages during an extended period in detumble mode lead to rests of varying frequency.

time the spacecraft apparently stabilized into a rotation about an axis that had the solar sail permanently shadowing the solar panels.* Reboots repeated on the order of minutes and the low power set the spacecraft clock back to its date of manufacture. Fortunately, once the memory issue was resolved, LightSail 2 was able to accept a transition into mode 2 and maneuver away from this attitude to recharge the batteries.

Several software updates were uplinked in November to prevent such situations in the future. To reduce power draw, a patch was applied to LightSail 2's cameras to deactivate their internal heater. The cameras are now heated by simply cycling their power any time their temperature drops below −10 C, a strategy that has proven effective both in reducing power and keeping the cameras in a reasonable temperature range. A second update has made time-tagged commands for mode transitions persistent across reboots. This prevents a reboot during momentum dumping from clearing the command to transition back to solar sailing once the momentum dump is complete. This is expected to reduce the chance of the spacecraft becoming stuck in detumble mode for extended periods of time.

VI. Conclusion

Solar sails are the oldest scientifically-grounded concept for space travel and they remain of great interest due to their propellantless method of spacecraft propulsion. While solar sails have been imagined for centuries, the first demonstrations did not occur until less than a decade ago. Created by The Planetary Society through the support of tens of thousands of supporters worldwide, LightSail 2 represents a crucial advancement of CubeSat solar sail technology. By successfully controlling the orientation of its sail relative to the Sun, the spacecraft has affected changes to the eccentricity of its orbit and the rate of orbital decay. This paper has provided a detailed analysis of major aspects of attitude determination and control, including validation through on-orbit testing and results from solar sailing. The success of this mission further demonstrates the readiness and potential of solar sail technology for future space missions. To aid those that follow, we summarize the most important lessons learned.

A. Lessons Learned
- *Solar panels on both sides of the solar sail*: Unlike LightSail 1, LightSail 2 did not have a solar panel on the +Z face of the spacecraft. In its place is a retro-reflector for precision laser ranging and orbit determination. Attempts at laser ranging have yet to be successful enough for orbit determination. As noted in Section V.B, the lack of solar panels on both sides of the sail has occasionally led to problems with power generation due to shadowing. Therefore, we recommend future missions include solar cells on both sides of the sail.
- *Higher altitudes*: Solar sail deployment drastically lowered LightSail 2's ballistic coefficient. At 720 km altitude the atmospheric drag has generally reduced orbit energy even when the on-off control strategy is being successfully

---

*As indicated by consistently cold ($< −30$ C) temperatures on the -Z panel and high (> 70 C) temperatures on the +Z panel

17

followed. Solar sails are better-suited to higher orbits or interplanetary missions where atmospheric drag is negligible.

- *Regular momentum dumping*: A key step in improving LightSail 2's attitude performance was instituting daily momentum dumps for 2 orbits. This improved pointing accuracy even when the momentum wheel had not yet saturated. Adding a brief no-torques period to demagnetize the torque rods also appeared to improve attitude control.

- *Inertial pointing mode*: Though not directly relevant to LightSail 2's mission objectives, an inertial pointing mode would have aided on-orbit validation of ADCS by providing a known and constant attitude for the spacecraft to follow.

B. On-going Activities

At the time of writing the spacecraft continues to be in good health. In addition to on-going solar sailing, an inertial sun-pointing mode is being developed to provide a comparison to the on-off strategy. Based on pre-launch estimates, LightSail 2 is expected to de-orbit in August of 2020. As the spacecraft descends, the mission will also provide a drag sail experiment. We plan to use LightSail 2's attitude control capability to modify the de-orbit timeline by changing the angle of the sail to the relative wind.

Acknowledgments

References

[1] Friedman, L. D., "The Story of LightSail," , 2015. URL https://www.planetary.org/explore/projects/lightsail-solar-sailing/story-of-lightsail-part-1.html.

[2] Johnson, L., Whorton, M., Heaton, A., Pinson, R., Laue, G., and Adams, C., "NanoSail-D: A solar sail demonstration mission," *Acta Astronautica*, Vol. 68, No. 5, 2011, pp. 571 – 575. https://doi.org/https://doi.org/10.1016/j.actaastro.2010.02.008.

[3] "Achievement of IKAROS — Japanese deep space solar sail demonstration mission," *Acta Astronautica*, Vol. 82, No. 2, 2013, pp. 183 – 188. https://doi.org/https://doi.org/10.1016/j.actaastro.2012.03.032.

[4] Vulpetti, G., Johnson, L., and Matloff, G. L., "The NanoSail-D2 NASA Mission," *Solar Sails: A Novel Approach to Interplanetary Travel*, Springer New York, New York, NY, 2015, pp. 173–178.

[5] Betts, B., Nye, B., Vaughn, J., Greeson, E., Chute, R., Spencer, D. A., Ridenoure, R. W., Munakata, R., Wong, S. D., Diaz, A., et al., "Lightsail 1 mission results and public outreach strategies," *The 4th International Symposium on Solar Sailing*, Kyoto Research Park, Kyoto, Japan, 2017.

[6] Plante, B. A., Spencer, D. A., Betts, B., Chait, S., Bellardo, J. M., Diaz, A., and Pham, I., "LightSail 2 ADCS: From Simulation to Mission Readiness," *The 4th International Symposium on Solar Sailing*, Kyoto Research Park, Kyoto, Japan, 2017.